

5-19-2009

Gate Induced g-factor Control and Dimensional Transition for Donors in Multi-Valley Semiconductors

Rajib Rahman

Purdue University - Main Campus

Seung H. Park

Purdue University - Main Campus

Timothy B. Boykin

The University of Alabama Huntsville

Gerhard Klimeck

Purdue University - Main Campus, gekco@purdue.edu

Sven Rogge

Delft University of Technology

See next page for additional authors

Follow this and additional works at: <http://docs.lib.purdue.edu/nanopub>

Rahman, Rajib; Park, Seung H.; Boykin, Timothy B.; Klimeck, Gerhard; Rogge, Sven; and Hollenberg, Lloyd C. L., "Gate Induced g-factor Control and Dimensional Transition for Donors in Multi-Valley Semiconductors" (2009). *Birck and NCN Publications*. Paper 427.

<http://docs.lib.purdue.edu/nanopub/427>

This document has been made available through Purdue e-Pubs, a service of the Purdue University Libraries. Please contact epubs@purdue.edu for additional information.

Authors

Rajib Rahman, Seung H. Park, Timothy B. Boykin, Gerhard Klimeck, Sven Rogge, and Lloyd C. L. Hollenberg

Gate induced g-factor control and dimensional transition in multi-valley semiconductors

Rajib Rahman,¹ Seung H. Park,¹ Timothy B. Boykin,² Gerhard Klimeck,^{1,3} Sven Rogge,⁴ and Lloyd C. L. Hollenberg⁵

¹Network for Computational Nanotechnology, Purdue University, West Lafayette, IN 47907, USA

²University of Alabama, Huntsville, AL 47907, USA

³Jet Propulsion Laboratory, California Institute of Technology, Pasadena, CA 91109, USA

⁴Kavli Institute of Nanoscience, Delft University of Technology, Delft, The Netherlands

⁵Center for Quantum Computer Technology, School of Physics, University of Melbourne, VIC 3010, Australia

(Dated: May 19, 2009)

The dependence of the g-factors of semiconductor donors on applied electric and magnetic fields is of immense importance in spin based quantum computation and in semiconductor spintronics. The donor g-factor Stark shift is sensitive to the orientation of the electric and magnetic fields and strongly influenced by the band-structure and spin-orbit interactions of the host. Using a multi-million atom tight-binding framework the spin-orbit Stark parameters are computed for donors in multi-valley semiconductors, silicon and germanium. Comparison with limited experimental data shows good agreement for a donor in silicon. Results for gate induced transition from 3D to 2D wave function confinement show that the corresponding g-factor shift in Si is experimentally observable.

PACS numbers: 71.55.Cn, 03.67.Lx, 85.35.Gv, 71.70.Ej

Understanding the behavior of single donor electron bound states under mesoscopic electric and magnetic fields is a fundamental issue critical to current miniaturization of semiconductor devices [1] and to the development of new quantum technologies [2, 3, 4]. It is only very recently that convergence between experiment and theory has occurred for the electric gate control of the orbital states [1] and electron-nuclear hyperfine interaction [5, 6] for a donor in silicon. However, the Stark shift of the donor spin-orbit interaction, which is central to understanding the precise spin properties in combined electric and magnetic fields, is just beginning to be understood [7]. We report the first atomistic treatment of the donor spin-orbit interaction in multi-valley semiconductors in gated environments, and show non-trivial agreement with experiment where available. We calculate the donor g-factor shift for the transition from 3D Coulomb to 2D interface confinement and show that the effect is experimentally observable.

Wave function engineering of donor spins is a basic ingredient of several quantum computing schemes [2, 3, 4], and may also help realize novel devices based on spin degrees of freedom. In one method, an applied E-field deforms the donor wave function and modifies its orbital angular momentum, which in turn can modify its spin properties through the spin-orbit interaction. This spin-orbit Stark effect is manifested by an E-field dependence of the effective g-factor, and can be probed by ESR experiments [5]. However, as we are dealing with donor levels in the solid-state, generally with complicated multi-valley orbital-spin effects, the physical origins of this phenomenon is at present not well understood. In semiconductors with significant spin-orbit interaction, this technique can even provide a way to rotate spins by electrical modulation of the g-tensor, and was demonstrated in

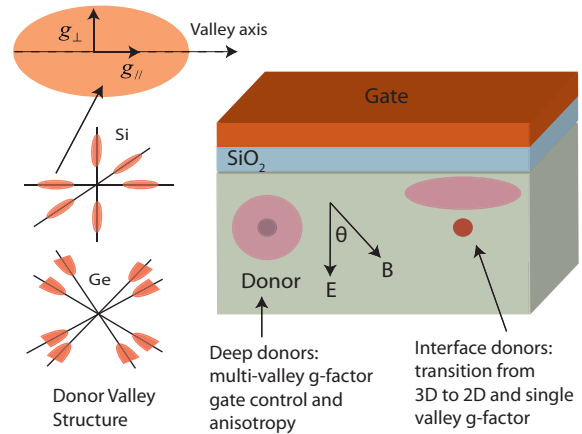


FIG. 1: Wave function and g-factor engineering of donor and interface confined electrons by EM fields in Si and Ge semiconductors (CB equivalent energy surfaces shown left).

GaAs quantum dots [8] and in GaAs/ $\text{Al}_x\text{Ga}_{1-x}\text{As}$ heterostructures [9, 10]. While the spin-orbit interaction in Si is relatively small, in a quantum computer application such effects can lead to qubit errors at the threshold level and need to be characterized and understood.

In this letter we report the first investigation of the Stark shift of the donor g-factor in two multi-valley semiconductors with varying degrees of spin-orbit interaction. We quantify the way in which the E-field removes the isotropy of the donor g-tensor components, resulting in an anisotropic Zeeman interaction. We also compare our g-factor Stark shift for P donors in Si against the only available measured value [5], and report corresponding parameters for Ge host under different orientations of E and B fields, as a guide for future experiments. Finally, we investigate g-factors of donors close to an oxide semiconductor interface, and study the g-factor variation as

the electron undergoes a symmetry transition from 3D Coulomb to 2D interfacial confinement [1]. This transition is central to proposals for donor-gate-confined interfacial transport and qubits in Si [11, 12].

Engineering the magnetic field response in semiconductors typically involves compound structures such as $\text{Al}_x\text{Ga}_{1-x}\text{As}$ or $\text{Si}_x\text{Ge}_{1-x}$ with a spatially varying material composition. Since the two materials, Al and Ga in $\text{Al}_x\text{Ga}_{1-x}\text{As}$ for example, have different g-factors, the effective g-factor of an electronic wave function can be controlled by pulling the wavefunction from an Al-rich part of the device to the Ga-rich part by means of an E-field [3]. The direct dependence of the g-factor on the field, however, has been largely ignored in literature except for Refs [10], where the g-tensor modulation resonance was used in $\text{Al}_x\text{Ga}_{1-x}\text{As}$ hetero-structures to control spin coherence electrically. In Ref [14], an all electrical control of the spin of a Mn hole in GaAs was investigated. A large anisotropic Zeeman splitting has been reported for acceptor levels in SiGeSi quantum wells [15] and also for single quantum states of nanoparticles [16]. Past ESR experiments [17, 18] have investigated the effect of uniaxial strain on donor g-factors in Si and Ge, while a recent work demonstrated the gate control of spin-orbit interaction in a GaAs/AlGaAs quantum well [19].

In this work, we employed an atomistic tight-binding (TB) theory with a 20 orbital $sp^3d^5s^*$ basis per atom including nearest neighbor and spin-orbit (SO) interactions. The total Hamiltonian of the host and the donor under an applied E-field can be expressed as,

$$H = H_0 - \frac{\hbar}{4m_0^2c^2} \vec{\sigma} \cdot \vec{p} \times \vec{\nabla} V_0 + U_{\text{donor}}(r) + e\vec{E} \cdot \vec{r}. \quad (1)$$

The first term represents the host semiconductor, the second term the SO interaction of the host due to the crystal potential V_0 , the third and the fourth represent the donor potential and the applied E-field. The semi-empirical TB parameters for Si and Ge [20, 21] used here have been well established in literature. The SO interaction of the host was represented as a matrix element between the p orbitals of the same atom after Chadi [22], and has been shown to cause energy splitting between the split-off hole (SH) band and the degenerate manifold of the light (LH) and heavy (HH) hole bands. This representation includes both the Rashba and Dresselhaus terms inherently, as opposed to the k-p method where the two are separately expressed. The donors are represented by a Coulomb potential screened by the dielectric constant of the host. The potential at the donor site U_0 was adjusted to obtain the ground state (GS) binding energy [23] taking into account the valley-orbit interaction in multi-valley semiconductors [24]. The total Hamiltonian was solved by a parallel Block Lanczos algorithm to obtain the relevant donor states. A typical simulation involved about 3 million atoms, and requires about 5 hours on 40 processors. The Zeeman Hamiltonian was

then evaluated perturbatively, using the matrix elements $H_{Zij} = \langle \Psi_i(\vec{r}, \vec{E}) | (\vec{L} + 2\vec{S}) \cdot \vec{B} | \Psi_j(\vec{r}, \vec{E}) \rangle$, where i, j represent \uparrow and \downarrow spins of a donor state. The small B-field (1T) used throughout this work justified the inclusion of linear B-field dependencies only in the Zeeman Hamiltonian. The g-factor was then evaluated using the lowest spin states (ϵ), $g(\vec{E}, \vec{B}) = (\epsilon_{\uparrow} - \epsilon_{\downarrow})/\mu_B|\vec{B}|$.

This TB model has been previously used to investigate the Stark shift of the hyperfine constant for a P donor in Si [6] in good agreement with ESR measurements [5] and momentum space methods [13]. It has also been successfully applied to interpret orbital Stark shift measurements on single As donors in Si FinFETS [1].

The g-factor for a donor ground state in a multi-valley semiconductor is influenced by two main factors. Within a single valley, the g-factor of electrons moving parallel to the valley axis ($g_{||}$) is different from the g-factor for perpendicular motion (g_{\perp}), assuming the semiconductor has non-spherical energy surfaces. This anisotropy may be affected further by external perturbations such as strain or E-fields, which may cause higher lying conduction bands (CB) to admix with the lowest CB [18]. Secondly, the donor ground states in Si and Ge have an equal admixture of all the valleys due to the valley-orbit interaction [24], resulting in an isotropic effective g-factor. Since an E-field removes the equivalency of the valleys, the effective g-factor becomes anisotropic depending on the contribution of the different valleys to the quantum state. The first effect is termed as the single-valley effect while the second the valley repopulation effect [17]. In a tight-binding description, it is not necessary to single out different valley contributions since the full band structure is considered in the formalism. Hence both effects are captured in the resulting g-factor.

TABLE I: Comparison of the quadratic g-factor Stark shift coefficient for donors in Si and Ge under different orientation of electric and magnetic fields.

Donor (valleys) [direction]	Valence band splitting [eV]	Binding energy [meV]	E-field	B-field	η_2 [$10^{-3} \mu\text{m}^2/V^2$]	
					Theory	Expt [5]
Si:P (6) [100]	0.044	-45.6	[010]	$B_{ }$	-0.012	-0.01 (Si:Sb)
				B_{\perp}	0.014	
Ge:P (4) [111]	0.29	-12.8	[010]	$B_{ }$	-4.8	-
				B_{\perp}	-4.8	
			[111]	$B_{ }$	143.8	
				B_{\perp}	-80.1	

Table I compares the spin-orbit properties of donors in Si and Ge. The SO interaction is stronger in Ge than in Si, as shown by the spin-orbit interaction whose strength is shown by the energy splitting of the split-off valence band from the degenerate light and heavy hole bands at the gamma point of its band structure. Si and Ge are multi-valley semiconductors with valleys located along [100] and [111] crystal axes respectively.

Fig 2 shows that the g-factor of donors primarily varies quadratically with the E-field. The g-factor shifts are af-

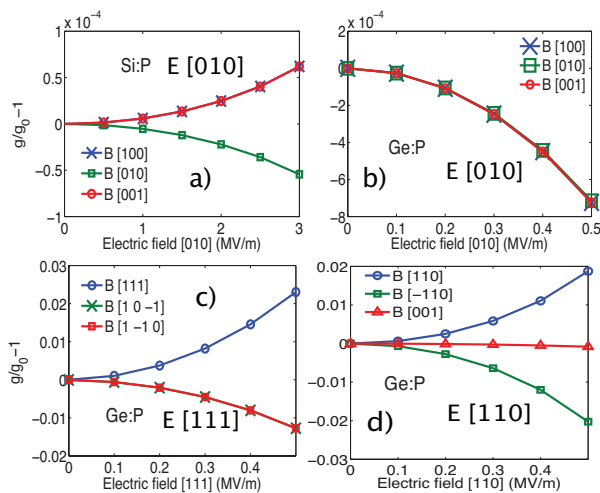


FIG. 2: Relative change in the the donor g-factor in Si and Ge as a function of E-field strength (in applied direction) and for parallel and perpendicular magnetic field orientation. a) Si:P under [010] E-field, b) Ge:P under [010] E-field, c) Ge:P under [111] E-field, and d) Ge:P under [110] E-field. The g-factor shift is sensitive to the relative orientation of the E and B fields with respect to the valley axis.

ected by the relative angles between the E-field, the valley axis, and the B-field. Fig 2a shows the g-factor of a P donor in Si subjected to [010] E-fields, while 2 b, c, and d are for a P donor in Ge under various orientations of the E-field. In Si the [010] E-field (2a) removes the equivalency of the six valleys, introducing the valley-repopulation effect in the donor wavefunction. This results in two different parabolas for the g-factor shifts, one for B parallel to E and the other for perpendicular orientation. The [010] directed E-field cannot remove the equivalency of the [111] valleys in Ge, and both parallel and perpendicular B-fields produce the same g-factor shifts (2b). However, when the field is directed along the [111] valley axis as in 2c, we obtain the split g-factor parabolas (2b) similar to Fig 2a. In the absence of an E-field, the Zeeman effect of the donor ground state is isotropic as shown by the convergence of the two parabolas at $E = 0$ in both Figs 2a and 2c.

The results of Fig 2 are fitted to a quadratic equation $g(E)/g(0) - 1 = \eta_2 E^2$, where η_2 is the quadratic Stark coefficient. Values of η_2 are shown in Table I for a few different E and B field orientations. For donors close to interfaces, there can be some linear Stark effect as well, which we discuss briefly in Fig 4. The quadratic coefficient of Si:P is of the order of $10^{-5} \mu\text{m}^2/\text{V}^2$, and compares well in magnitude with the only available experimental data on Si:Sb. Order of magnitude comparison of η_2 for Si and Ge shows that the spin-orbit Stark effect is stronger in Ge than in Si. The Zeeman anisotropy is also stronger for donors in Ge, where the quadratic coefficients can differ by an order of magnitude between parallel and perpendicular B-fields (Table 1). The direction of the E-field relative to the valley-axes also affects

the strength of the Zeeman interaction. This is shown by comparing the B_{\parallel} results of Ge:P for [010] and [111] directed E-fields. The quadratic Stark coefficients in this case differ by two orders of magnitude. Our results show very good agreement in magnitude of η_2 for Si:P with the measured value reported in Ref [5], however, there is a discrepancy regarding the relative sign of the g-factor shift in the quadratic regime which we are currently unable to account for. Within the TB framework calculations of the g-factor Stark shift for the single valley GaAs case were also carried out and showed good agreement in magnitude in comparison with the recent k.p results [7].

A simple multi-valley picture provides some intuitive explanations of the Stark shifted g-factor based on the valley repopulation effect. If $|a_x|^2$ represents the contribution of the $+x$ valley in Si to the donor GS, and g'_{+x} the diagonal g-tensor corresponding to this valley with the x component given by g_{\parallel} while the y and z components given by g_{\perp} , then the effective g-tensor of the donor GS is given by $g(E) = \sum_{i=\pm x, \pm y, \pm z} |a_i|^2 g'_i$. Assuming $a_i = a_{-i}$ and $a_x = a_z$ for a [010] E-field, we obtain the effective g-tensor components g_x , g_y and g_z as,

$$g_x = g_z = 2(|a_y|^2 + |a_x|^2)g_{\perp} + 2|a_x|^2g_{\parallel} \quad (2)$$

$$g_y = 4|a_x|^2g_{\perp} + |a_y|^2g_{\parallel} \quad (3)$$

These equations show that the parallel component of the g-factor has a different response to the electric field as compared to the perpendicular component, verifying the split g-factor curves of Fig 2a and 2d. At $E = 0$, each $a_i = 1/\sqrt{6}$, and eqs (2) and (3) reduce to $g_x = g_y = g_z = \frac{2}{3}g_{\perp} + \frac{1}{3}g_{\parallel} = g_0$, showing an isotropic effective g-factor. At ionizing E-fields, only the valleys parallel to the field contribute to the state. Setting $a_y = 1/\sqrt{2}$ and $a_x = a_z = 0$ in (2) and (3), $g_x = g_{\perp}$ and $g_y = g_{\parallel}$, which helps to probe the single valley g-factors, as shown later in Fig 4. Similar expressions can be derived for a donor in Ge taking into account that the Ge valleys are in [111]. For a more quantitative approach, however, one needs to know also the g-factor variation within a single valley, the precise nature of the wavefunction distortion by the E-field, and the effect of B-fields. The TB approach provides a generalized framework to include all these.

In Fig 3, we vary the angle θ between the E and B-fields from 0 to 90 degrees for a) Si:P under [010] E-field, and b) Ge:P under [111] E-field. The relative change in g-factor shows a linear dependence on $\sin^2 \theta$, consistent with Ref [18]. The sensitivity of this variation increases at higher E-fields as shown in Fig 3a and 3b. The flat $E = 0$ line indicates that the Zeeman effect is isotropic at zero field. Assuming an y-directed E-field in Si such that the effective g-tensor diagonal components are given by $g_x(E) = g_z(E) \neq g_y(E)$, the linear dependence of $g(E)$ on $\sin^2 \theta$ is shown by,

$$g(E) \approx g_y(E) \left(1 + \frac{g_x(E)^2 - g_y(E)^2}{2g_y(E)^2} \sin^2 \theta \right) \quad (4)$$

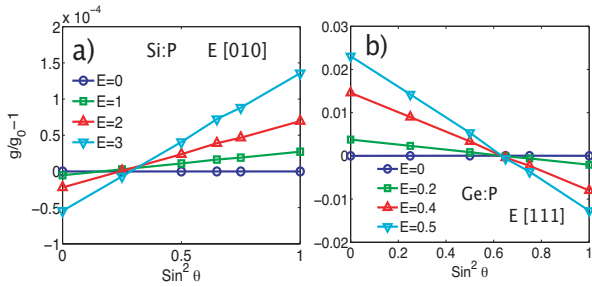


FIG. 3: Anisotropic Zeeman effect with E-field. θ represents the angle between the E and the 1T B field. a) Si:P under [010] E-field with B-field varying from [010] to [001]. b) Ge:P under [111] E-field, with B-field varying from [111] to [1-10].

Eq 4 can be derived by expanding $g = (g_y(E)^2 \cos^2 \theta + g_x(E)^2 \sin^2 \theta)^{1/2}$ up to linear terms in $(g_x(E)^2/g_y(E)^2 - 1) \sin^2 \theta$.

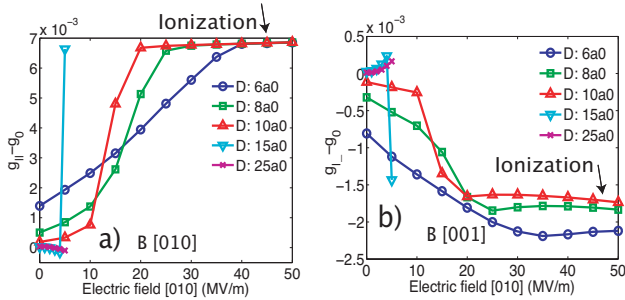


FIG. 4: Interface effects on the donor g-factor for Si:P. g-component a) parallel, b) perpendicular to the field and the interface at various donor depths.

The confinement transition from 3D Coulomb to an interface 2D system has recently been observed (in conjunction with the theoretical approach used here) [1], and is related to a new control scheme based on dopants close to the Si-SiO₂ interface [11]. The donor electron can be adiabatically pulled to the interface by gate voltages [13, 25, 26], and controlled by surface gates. We computed the g-factor of a system undergoing this confinement transition. Fig 4 shows the components of the g-factor parallel (4a) perpendicular (4b) to the E-field for various donor depths. As the E-field increases, the two Si conduction band valleys in the direction of the field are lowered in energy relative to the four valleys perpendicular to the field axis. The interface state realized at ionizing E-fields has contribution from these two uni-axial valleys, and hence their $g_{||}$ and g_{\perp} approach those of the two valleys. Our simulations indicate $g_{||} - g_{\perp} \approx 8 \times 10^{-3}$, which compares well in order of magnitude with the measurements of Ref [18]. This g-factor anisotropy has also been reported in 2DEGS [27]. The transition to the single valley g components is abrupt if the donor is far away from the interface (>10 nm), and gradual if the donors are closer to the interface [13, 25, 26]. Proximity to interfaces is also marked by linear Stark effect since the wave

function becomes asymmetric due to sharp truncation by the surface. Fig 4 shows at small donor depths, the $g_{||}$ and g_{\perp} also exhibit a linear field dependence. In this regime, the linear Stark coefficient exceeds the quadratic coefficient. A similar effect was observed for the hyperfine Stark effect [6].

In conclusion, we have for the first time applied atomistic techniques to understand and predict the E-field response of donor g-factors in multi-valley (Si, Ge) semiconductors with different degrees of spin-orbit interaction. The E-field induces a Zeeman anisotropy that varies with the relative angle between the E and the B fields. The strength of the Stark shift is also dependent on the direction of the E-field relative to the valley axis. The computed Stark shift coefficient of Si:P compares well in magnitude with the only available measured value for donors in Si. The donor g-factor Stark shift was also computed for the 3D to 2D confinement transition, suggesting that the effect is accessible to experiments.

This work was supported by the Australian Research Council, NSA and ARO (contract number W911NF-04-1-0290). Part of the development of NEMO-3D was performed at JPL, Caltech under a contract with NASA. NCN/nanohub.org computer resources were used.

Electronic address: rrahman@purdue.edu

- [1] G. P. Lansbergen *et al.*, Nature Physics **4**, 656 (2008).
- [2] B. E. Kane, Nature, **393**, 133 (1998).
- [3] R. Vrijen *et al.*, Phys. Rev. A **62**, 012306 (2000).
- [4] L. Hollenberg *et al.*, Phys. Rev. B **69**, 113301 (2004).
- [5] F. R. Bradbury *et al.*, Phys Rev. Lett. **97**, 176404 (2006).
- [6] R. Rahman *et al.*, Phys Rev. Lett. **99**, 036403 (2007).
- [7] A. De *et al.*, Phys Rev. Lett. **102**, 017603 (2009).
- [8] K. C. Nowack *et al.*, Science, **318**, 1430 (2007).
- [9] Y. Kato *et al.*, Science **299**, 1201 (2003).
- [10] G. Salis *et al.*, Nature (London) **414**, 619 (2001).
- [11] M.J. Calderon *et al.*, Phys. Rev. Lett. **96**, 096802 (2006).
- [12] A. J. Skinner *et al.*, Phys. Rev. Lett. **90**, 087901 (2003).
- [13] C. Wellard and L. Hollenberg, Phys. Rev. B **72**, 085202 (2005).
- [14] J. M. Tang *et al.*, Phys. Rev. Lett. **97**, 106803 (2006).
- [15] K.-M. Haendel *et al.*, Phys. Rev. Lett. **96**, 086403 (2006).
- [16] J. R. Petta and D. C. Ralph, Phys Rev. Lett. **89**, 156802 (2002).
- [17] L. Roth, Phys. Rev. **118**, 1534 (1960).
- [18] D. K. Wilson and G. Feher, Phys. Rev. **124**, 1068 (1961).
- [19] M. Studer *et al.*, arxiv:0903.092v1 (2009).
- [20] T. B. Boykin *et al.*, Phys. Rev. B **69**, 115201 (2004).
- [21] G. Klimeck *et al.*, Comp. Model. Eng. Sci. **3**, 601, (2002).
- [22] D. J. Chadi, Phys. Rev. B **16**, 790 (1977).
- [23] S. Ahmed *et al.*, Encycl. of Complexity of Systems (2008).
- [24] W. Kohn and J. M. Luttinger, Phys. Rev. **98**, 915 (1955).
- [25] A. S. Martins *et al.*, Phys. Rev. B **69**, 085320 (2004).
- [26] G. Smit *et al.*, Phys. Rev. B **70**, 035206 (2004).
- [27] R. Winkler *et al.*, Phys Rev. Lett. **85**, 4574 (2000).